Experimental demonstration of programmable multi-functional spin logic cell based on spin Hall effect

CrossMark

X. Zhang, C.H. Wan[*], Z.H. Yuan, C. Fang, W.J. Kong, H. Wu, Q.T. Zhang, B.S. Tao, X.F. Han[*]

Beijing National Laboratory for Condensed Matter Physics, Institute of Physics, University of Chinese Academy of Sciences, Chinese Academy of Sciences, Beijing 100190, China

ARTICLE INFO

ABSTRACT

Confronting with the gigantic volume of data produced every day, raising integration density by reducing the size of devices becomes harder and harder to meet the ever-increasing demand for high-performance computers. One feasible path is to actualize more logic functions in one cell. In this respect, we experimentally demonstrate a prototype spin-orbit torque based spin logic cell integrated with five frequently used logic functions (AND, OR, NOT, NAND and NOR). The cell can be easily programmed and reprogrammed to perform desired function. Furthermore, the information stored in cells is symmetry-protected, making it possible to expand into logic gate array where the cell can be manipulated one by one without changing the information of other undesired cells. This work provides a prospective example of multi-functional spin logic cell with reprogrammability and nonvolatility, which will advance the application of spin logic devices.

1. Introduction

Spin logic is of great interest as its desired property of nonvolatility and subsequentially the potential for realizing the idea of processing in memory architecture which is regarded to play increasingly important role in today's fast-growing volumes of data. Many efforts have been dedicated to explore the prospective candidates of spin logic gate in different systems such as semiconductors [1,2], Oersted-field controlled magnetic tunnel junctions [3], magnetic domain engineered nanowires [4], phase-change material [5], graphene [6,7] and magnetoelectric oxides [8]. However, only a few of them are compatible with complementary metal oxide semiconductor (CMOS) architecture, which limits their practical applications. On the other hand, confronted with huge volumes of data, the demand for high-performance computer naturally becomes an urgency. The traditional solution guided by Moore's law is to miniaturize logic device so as to increase the total number of logic gates, which, however, is hampered by the physical and lithographic restrictions [9–11]. One feasible path is to integrate different logic functions into a single cell, which is nearly impossible for current silicon-based logic device [11]. In this regard, the interplay between orbit and spin has provided new possibilities for electrical manipulation of magnetization. The magnetization switching based on the spin-orbit torques (SOT) induced by spin Hall effect (SHE) has been demonstrated in heavy metal/ferromagnet heterostructures not only with in-plane anisotropy [12,13] but with perpendicular aniso-

tropy [14–18].

Here, we experimentally demonstrate a prototype spin logic cell integrated with five Boolean functions (AND OR NOT NAND and NOR) in perpendicularly magnetized Pt/Co/MgO system. The spin logic cell can be programmed between different logic functions by changing the direction of magnetic field and initial magnetic state. By carefully arranging experimental setup, the robustness of the information stored in cells is intrinsically guaranteed by the symmetry requirements of SOT-induced magnetization switching. This work provides a promising candidate for highly integrated multi-functional spin logic cell with programmability and compatibility with current CMOS architecture.

2. Results

As-deposited Pt(5)/Co(0.8)/MgO(2)/Pt(2) stacks (thickness in nm) have in-plane easy axis which gradually reorients normal to the film plane after annealing above 250 °C under a 7 kOe perpendicular magnetic field. The perpendicular anisotropy of our samples reaches maximum at annealing temperature of 400 °C. Further increase in annealing temperature will result in the degradation of PMA. The following data is based on samples after 400 °C annealing process in a perpendicular magnetic field. Hall measurement of the sample is shown in Fig. 1b. Sharp change of the anomalous Hall resistance R_{xy} was observed for the out-of-plane magnetic field, while it took over 6 kOe to saturate the magnetization for the in-plane field, which
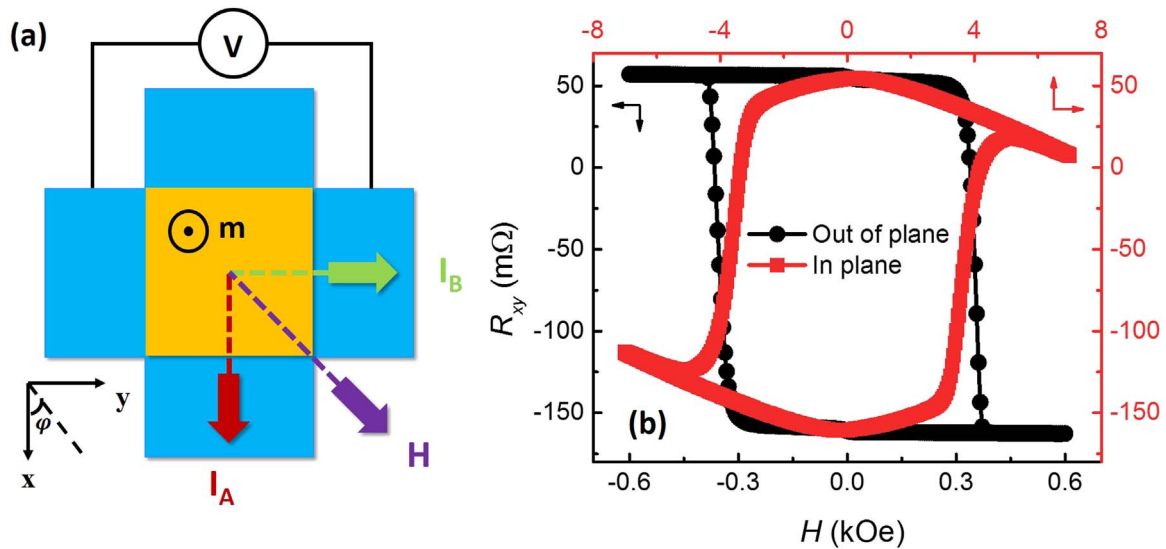
Fig. 1. Measurement setup and magnetic characterization (a) Schematic illustration of experimental setup. I_A is along x direction, I_B along y direction and H along the angle bisector of I_A and I_B. φ is the in-plane angle with respect to $+x$. (b) Hall measurement under out-of-plane field (black circle) and in-plane field (red square). (For interpretation of the references to color in this figure legend, the reader is referred to the web version of this article.)

confirms the perpendicular anisotropy of the samples.

The film was patterned into cells with cross-shaped Hall bar with $20*20$ μm^2 center region, as shown in Fig. 1a. Two currents with identical amplitude, I_A and I_B, which are orthogonal to each other, were applied simultaneously to destabilize the magnetic state of the cell. Then, a small I_A was applied as a read current to pick up the anomalous Hall resistance R_{xy}, which reveals the magnetic state of the system. An in-plane magnetic field H was applied along the angle bisector between I_A and I_B, i.e. $\varphi=45°$ for $H>0$ and $\varphi=225°$ for $H<0$. Fig. 2 plots the current-induced switching under different measurement conditions. Before the current sweeping, the system was initialized to $+m_z$ or $-m_z$. Two current configurations were utilized to perform the measurements i.e. I_A and I_B are applied with the same polarity ($I_A=I_B$ configuration) and with the opposite polarity ($I_A=-I_B$ configuration), and the definition of the current polarity is shown in Fig. 1a. Two distinct behaviors are manifested under two kinds of current configurations. For $I_A=I_B$ configuration, complete magnetization switching loop was observed, which is independent of initial magnetic state. The critical current is 50 mA and, importantly, the sequence of magnetic reversal process changed from clockwise to anti-clockwise when $H=-120$ Oe was switched to the opposite direction $H=+120$ Oe. On the other hand, for $I_A=-I_B$ configuration, the magnetic state follows its initial magnetization and remains unaffected by changing both the direction of H and the amplitude of applied currents within range of 55 mA.

Based on the different behaviors in two kinds of current configurations, we propose a prototype spin logic cell making use of this symmetry-dependent switching characteristics. Fig. 3 shows the logic performance of this spin logic cell. Five logic functions, i.e. OR, AND, NOR, NAND and NOT, are all realized in the same cell. I_A and I_B serve as two independent input channels and the operation currents are determined to be $+55$ mA for logic input 1 and -55 mA for logic input 0. The logic output is carried by magnetic state, which in turn is reflected by anomalous Hall resistance R_{xy}. For all five logic functions, the reference R_{xy} is designed to be -300 $m\Omega$ above which we define the logic output 1 ($+m_z$ state) and below which we define the logic output 0 ($-m_z$ state). We adopt two-step operation to execute a single logic test. The first step is initialization, that is, we set the cell to a certain initial state. The second step is logic operation. Four logic input combinations are applied one by one to the programmed cell to check the consistency with the truth tables.

For OR gate (Fig. 3a), H of $+1200$ Oe is applied and the magnetic state was initialized to $+m_z$ (logic '1' state) before each logic operation. For $I_A=I_B$ configuration, $+55$ mA, i.e. logic input (1, 1), will select $+m_z$ state leading to logic output 1, while -55 mA, i.e. logic input (0, 0), will reverse the state to $-m_z$, giving logic output 0. For $I_A=-I_B$ configuration, both logic input (1, 0) and (0, 1) cannot drive the cell away from its initial state $+m_z$, exporting logic 1.

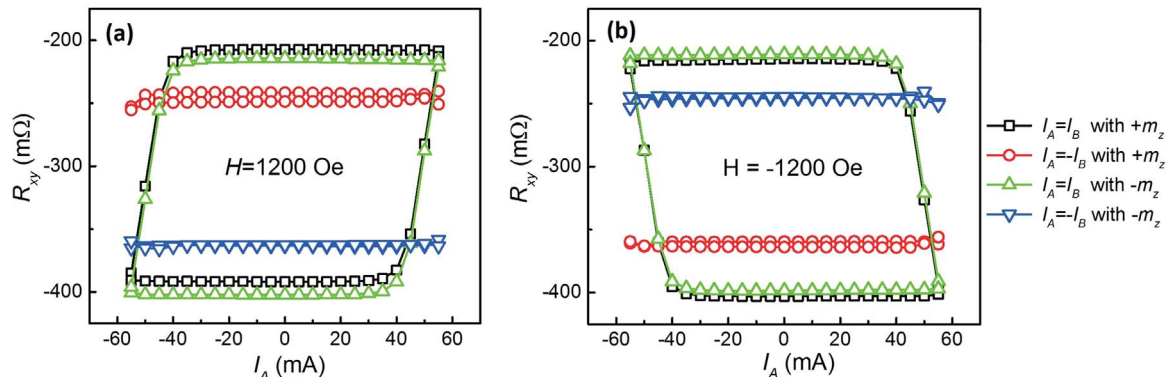For AND gate (Fig. 3b), the same H is applied. The only condition

Fig. 2. Current-induced magnetization switching measurements. (a) $H=1200$ Oe and (b) $H=-120$ Oe. For each magnetic field, $I_A=I_B$ configuration (black square and green up triangle) and $I_A=-I_B$ configuration (red circle and blue down triangle) were used. Before current sweeping, the system was initialized to $+m_z$ (black square and red circle) or $-m_z$ (green up triangle and blue down triangle). (For interpretation of the references to color in this figure legend, the reader is referred to the web version of this article.)
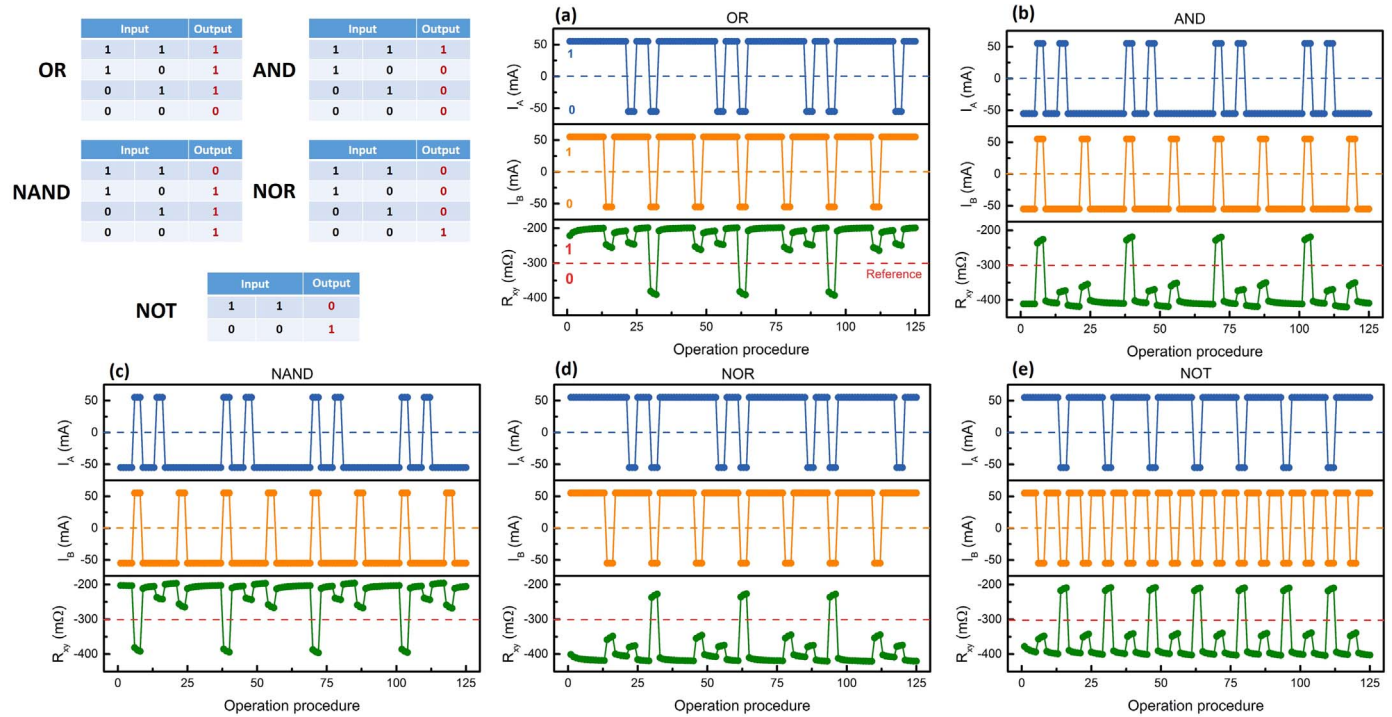
Fig. 3. Logic function test for a single spin logic cell. Five Boolean functions of (a) OR, (b) AND, (c) NAND, (d) NOR and (e) NOT are realized. I_A and I_B are served as input signal. 1 and 0 corresponds to positive and negative current, respectively. The reference value of output signal is −300 m Ω above which is defined as '1' and below which is defined as '0'. Truth table of these functions are shown at the very beginning.

needed to change in comparison with the OR gate is that the initial state is set to $-m_z$ (logic '0' state) before each logic operation. Therefore, for $I_A=I_B$ configuration, +55 mA leads to logic output 1, while −55 mA gives logic output 0, just the same as OR gate. However, for $I_A=-I_B$ configuration, the initialization ensures the logic output to be 0 for input (1, 0) and (0, 1).

For NOR gate (Fig. 3c), the magnetic state was initialized to $-m_z$ (logic '0' state) before each operation. In contrast with OR gate, the $H=-120$ Oe is adopted. Thus, for $I_A=I_B$ configuration, logic input (1, 1) will select $-m_z$ state leading to logic output 0, while logic input (0, 0) will reverse the state to $+m_z$, giving logic output 1. For $I_A=-I_B$ configuration, logic input of both (1, 0) and (0, 1) cannot change the magnetic state. Thus, the cell follows the initial state $-m_z$, exporting logic 0.

For NAND gate (Fig. 3d), the magnetic initial state was set to $+m_z$ (logic '1' state) before each operation. Similar to NOR gate, the H of −1200 Oe is applied. Therefore, for $I_A=I_B$ configuration, +55 mA leads to logic output 0, while −55 mA gives logic output 1. For $I_A=-I_B$ configuration, corresponding to logic input of both (1, 0) and (0, 1), the cell follows the initial state $-m_z$, exhibiting logic 0.

For NOT gate (Fig. 3e), H of −1200 Oe is applied and the magnetic state was initialized to $-m_z$. Here, I_A is used as the input channel, while I_B is fixed to −55 mA in each logic operation. As a result, I_A=+55 mA (logic input 1) cannot destabilize $-m_z$ state and the output is logic 0. In contrast, I_A=−55 mA (logic input 0) will make the magnetic state of cell switch to $+m_z$, giving logic output 1.

3. Discussion

The physical origin of switching characteristics under different current configurations can be understood through the symmetry requirement based on Landau-Lifshitz-Gilbert (LLG) equation [15,18,19]. Briefly, deterministic current-induced switching of perpendicularly magnetized films will occur if applied current is along the direction of in-plane magnetic field but will never be realized if the current is applied normal to the direction of magnetic field. Noting that

the crossing region experiences two channels of applied current with identical amplitude, i.e. j_A and j_B. Therefore, for $I_A=I_B$ configuration, total current density $j = j_A +j_B$ is along the direction of the angle bisector between I_A and I_B (φ=45°) which, in this work, is parallel or antiparallel to the direction of magnetic field. Deterministic current-induced switching can be expected. In contrast, for $I_A=-I_B$ configuration, total current density j is along the other direction of the angle bisector between I_A and I_B ($\varphi= -45$°) which is normal to the direction of magnetic field. Thus, magnetization cannot be switched to the opposite direction, making the initial magnetic state resist the destabilization of applied currents. It is worth the stress that this stability of initial state is symmetry-protected, which guarantees the robustness of the information stored in magnetic state.

It is worth mentioning that the magnetic state can be changed only for $I_A=I_B$ configuration, as shown above. This feature makes it convenient to expand the single cell to a gate array in which each cell can be manipulated one by one via two mutually orthogonal channels of current, as illustrated in Fig. 4a. In this consideration, the logic state of cells under a single current should not be changed so that only desired gates are controlled without the influence on the rest. Fig. 4 plots the response of the passing cells under a single current. Fig. 4b and c are initialized to $-m_z$ and $+m_z$, respectively. As can be seen, the initial magnetic state is insensitive to applied current regardless of H=+120 Oe or H=−120 Oe. As a result, the data stored in cells remain unaffected by a single current and in-plane magnetic field which provides the possibility of site-specific tunable gate array formed by these spin logic cells.

As for further application, the Pt/Co/MgO can be used as the free layer of a magnetic tunnel junction (MTJ) which has been widely applied in magnetic data storage and is well compatible with current CMOS architecture. The magnetic state in this way can be read via tunneling magnetoresistance (TMR) effect instead of AHE. This also leads to the separation of read and write operation, i.e. read operation is from TMR effect through the MTJ, while the write operation is from SHE only on the free layer regardless of the junction. This makes the spin logic cell meet the requirement of feedback prevention [20].
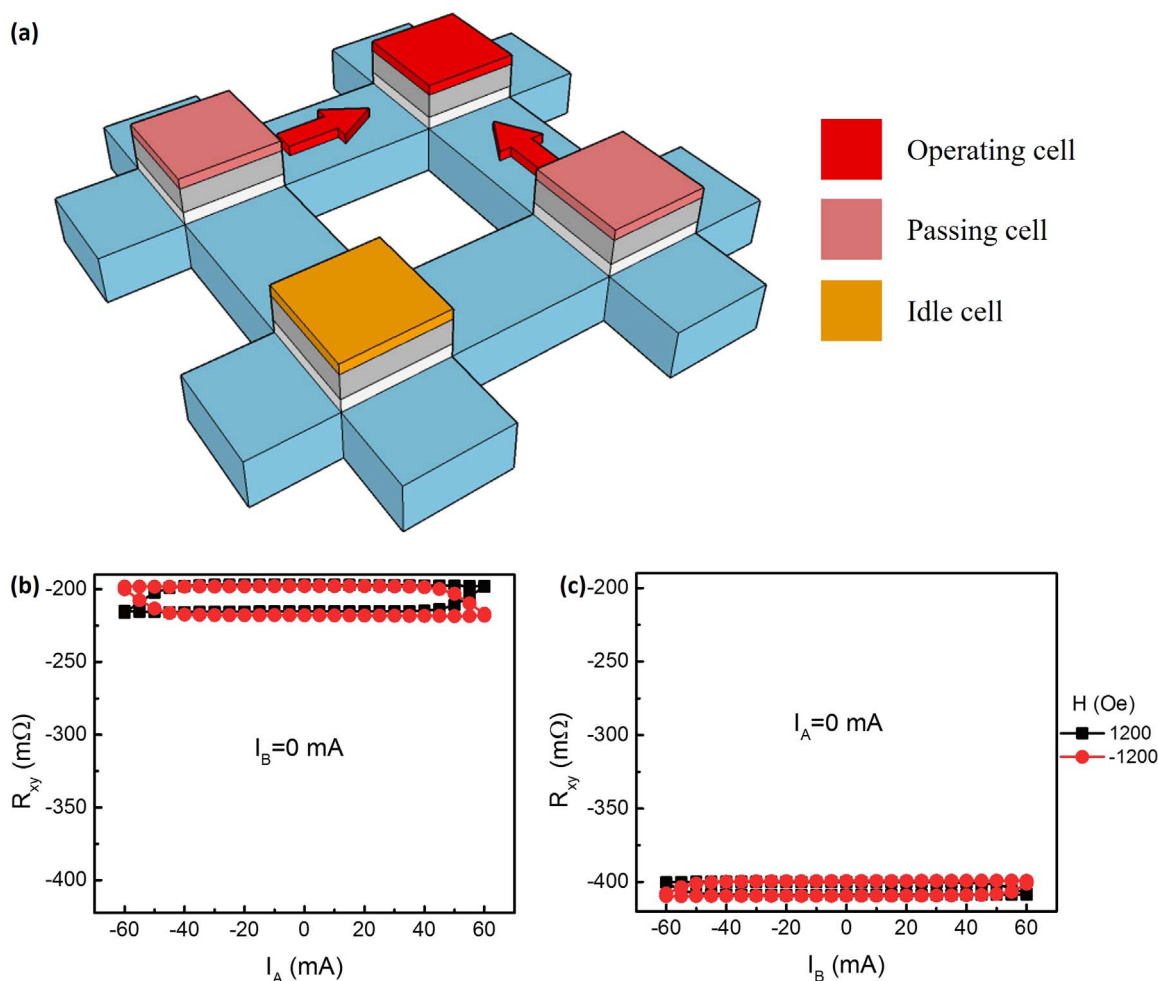
Fig. 4. Gate array draft and information robustness test of spin logic cell. (a) Schematic illustration of gate array formed by spin logic cells in this work. Operating cell (red), passing cell (pink) and idle cell (orange) are defined as the cell experiences two currents, one current and no current, respectively. Stability test for the passing logic cells which are under single current stimulation with (b) only I_A being applied and (c) only I_B being applied. Each test is performed twice under magnetic field of 1200 Oe (black square) and −1200 Oe (red circle). (For interpretation of the references to color in this figure legend, the reader is referred to the web version of this article.)

Meanwhile, the MTJ can output a large or small current corresponding to the logic state '1' or '0' stored in the free layer stemming from TMR effect and this current can be further used as an input current to the next nearby logic cell, which realizes the concatenability [20]. Technically speaking, there is no fundamental obstacle to prevent the size of MTJ down to sub-100 nm scale [21]. Moreover, it's been reported that the process of SHE-induced magnetization switching can be finished within 0.1–1 ns [22,23], which proves the capability of high-speed data processing.

In summary, by utilizing two mutually orthogonal currents and a specific magnetic field, two distinctive behaviors of magnetization with respect to two current configurations are observed. Based on aforementioned features, we proposed one possible prototype logic cell of spin logic application. Five typical logic functions (AND, OR, NAND, NOR and NOT) can be realized in a single spin logic cell. The logic function of the cell is determined by the polarization of magnetic field and the initial magnetic state and thus can be easily reprogrammed to perform an anticipated function. Moreover, the information stored in the cell is insensitive to the stimulation of a single current, which makes it possible to manipulate a specific cell in a gate array without destroying the data in undesired passing cells. This work provides a novel setup from conventional spin-Hall-torque-induced magnetization switching experiments and proposes a prototype spin logic cell that can serve as a promising candidate for future spin logic applications.

4. Materials and methods

Pt(5)/Co(0.8)/MgO(2)/Pt(3) samples (nominal thickness in nanometer) are provided by Singulus Technologies AG. They were deposited on Si/SiO$_2$ substrate by magnetron sputtering at room temperature. Co exhibited in-plane anisotropy in as-deposited state, while the easy axis reoriented perpendicular to film plane after over 150 °C annealing process with 0.7 T magnetic out-of-plane field. Ultraviolet lithography combined with two-step argon ion etching was utilized to pattern raw film into Hall bar with the dimension of center square region being 20 μm. Low-resistive Cu(10 nm)/Au(30 nm) was deposited as electrodes on four pad regions. The 4-terminal electrical measurements were performed with a current source (Keithley 2400) and a nanovoltmeter (Keithley 2182). The temperature control and magnetic field environment were provided by Physical Property Measurement System (PPMS-9T, Quantum Design). For current-induced magnetization switching and logic operation measurements, we adopted the following procedure. First, two stimulation currents pulse with fixed ratio, i.e. I_A and I_B with $I_A/I_B=k$, were applied simultaneously to change the magnetic state of sample. Second, a small current pulse was used as detection current to figure out the magnetic state after the stimulation.

References

[1] S. Datta, B. Das, Appl. Phys. Lett. 56 (1990) 665.
[2] H. Dery, P. Dalal, L. Cywinski, L.J. Sham, Nature 447 (2007) 573.
[3] A. Ney, C. Pampuch, R. Koch, K.H. Ploog, Nature 425 (2003) 485.
[4] D.A. Allwood, G. Xiong, C.C. Faulkner, D. Atkinson, D. Petit, R.P. Cowburn, Science 309 (2005) 1688.
[5] J. Borghetti, G.S. Snider, P.J. Kuekes, J.J. Yang, D.R. Stewart, R.S. Williams, Nature 464 (2010) 873.
[6] H. Wen, T. Zhu, Y. Luo, W. Amamou, R.K. Kawakami, J. Appl. Phys. 115 (2014) 17B741.
[7] W. Han, R.K. Kawakami, M. Gmitra, J. Fabian, Nat. Nanotech 9 (2014) 794.
[8] D.E. Nikonov, I.A. Young, J. Mater. Res. 29 (2014) 2109.
[9] C.P. Collier, E.W. Wong, M. Belohradský, F.M. Raymo, J.F. Stoddart, P.J. Kuekes, R.S. Williams, J.R. Heath, Science 285 (1999) 391.
[10] Y. Huang, X. Duan, Y. Cui, L.J. Lauhon, K.-H. Kim, C.M. Lieber, Science 294 (2001) 1313.
[11] D. Loke, J.M. Skelton, W.-J. Wang, T.-H. Lee, R. Zhao, T.-C. Chong, S.R. Elliott, Proc. Natl. Acad. Sci. 111 (2014) 13272.
[12] L. Liu, C.F. Pai, Y. Li, H.W. Tseng, D.C. Ralph, R.A. Buhrman, Science 336 (2012) 555.
[13] X. Fan, J. Wu, Y. Chen, M.J. Jerry, H. Zhang, J.Q. Xiao, Nat. Commun. 4 (2013) 1799.
[14] I.M. Miron, K. Garello, G. Gaudin, P.J. Zermatten, M.V. Costache, S. Auffret, S. Bandiera, B. Rodmacq, A. Schuhl, P. Gambardella, Nature 476 (2011) 189.
[15] L. Liu, O.J. Lee, T.J. Gudmundsen, D.C. Ralph, R.A. Buhrman, Phy. Rev. Lett. 109 (2012) 096602.
[16] S. Fukami, C. Zhang, S. DuttaGupta, A. Kurenkov, H. Ohno, Nat. Mater. 535 (2016).
[17] A. van den Brink, G. Vermijs, A. Solignac, J. Koo, J.T. Kohlhepp, H.J.M. Swagten, B. Koopmans, Nat. Commun. 7 (10854) (2016) 10854.
[18] X. Zhang, C.H. Wan, Z.H. Yuan, Q.T. Zhang, H. Wu, L. Huang, W.J. Kong, C. Fang, U. Khan, X.F. Han, Phys. Rev. B 94 (2016) 174434.
[19] G. Yu, P. Upadhyaya, Y. Fan, J.G. Alzate, W. Jiang, K.L. Wong, S. Takei, S.A. Bender, L.T. Chang, Y. Jiang, M. Lang, J. Tang, Y. Wang, Y. Tserkovnyak, P.K. Amiri, K.L. Wang, Nat. Nanotechnol. 9 (2014) 548.
[20] B. Behin-Aein, D. Datta, S. Salahuddin, S. Datta, Nat. Nanotechnol. 5 (2010) 266.
[21] S. Ikeda, K. Miura, H. Yamamoto, K. Mizunuma, H.D. Gan, M. Endo, S. Kanai, J. Hayakawa, F. Matsukura, H. Ohno, Nat. Mater. 9 (2010) 721.
[22] K. Garello, C.O. Avci, I.M. Miron, M. Baumgartner, A. Ghosh, S. Auffret, O. Boulle, G. Gaudin, P. Gambardella, Appl. Phys. Lett. 105 (2014) 212402.
[23] M. Sasikanth, E.N. Dmitri, A.Y. Ian, Appl. Phys. Express 7 (2014) 103001.